Beam Selection Algorithm Utilizing Fingerprint DB Based on User Types in UAV Support Systems

Jihyung Kim[1], Yuna Sim[2], Sangmi Moon[3], and Intae Hwang[4*]
[1]Spatial Wireless Transmission Research Section, Electronics and Telecommunications Research Institute,
218, Gajeong-ro, Yuseong-gu, Daejeon, 34129, Republic of Korea
[e-mail : savant21@etri.re.kr]
[2] Department of ICT Convergence System Engineering, Chonnam National University,
77, Yongbong-ro, Buk-gu, Gwangju, 61186, Republic of Korea
[e-mail : sya8325@naver.com]
[3] Department of IT Artificial Intelligence, Korea Nazarene University,
Wolbong-ro 48, Cheonan-city, Choongcheongnam-do, 31172, Republic of Korea
[e-mail : moonsm@kornu.ac.kr]
[4] Department of Electronic Engineering and Department of ICT Convergence System Engineering,
College of Engineering, Chonnam National University,
77, Yongbong-ro, Buk-gu, Gwangju, 61186, Republic of Korea
[e-mail : hit@jnu.ac.kr]
[*]Corresponding author: Intae Hwang

Received July 13, 2023; revised August 15, 2023; accepted August 26, 2023;
published September 30, 2023

Abstract

The high-altitude and mobility characteristics of unmanned aerial vehicles (UAVs) have made them a key element of new radio systems, particularly because they can exceed the limits of terrestrial networks. However, at high altitudes, UAVs can be significantly affected by intercell interference at a high line-of-sight probability. To mitigate this drawback, we propose an algorithm that selects the optimal beam to reduce interference and maximize transmission efficiency. The proposed algorithm comprises two steps: constructing a user-location-based fingerprint database according to the user types presented herein and cooperative beam selection. Simulations were conducted using cellular cooperative downlink systems for analyzing the performance of the proposed method, and the signal-to-interference-plus-noise cumulative distribution function and spectral efficiency cumulative distribution function were used as performance analysis indicators. Simulation results showed that the proposed algorithm could reduce the effect of interference and increase the performance of the desired signal. Moreover, the algorithm could efficiently reduce overheads and system cost by reducing the amount of resources required for information exchange.

Keywords: Cellular-connected system, cumulative distribution function, cooperative beam selection, fingerprint database, signal-to-interference-plus-noise ratio, spectral efficiency, unmanned aerial vehicle.

"This work was supported by Electronics and Telecommunications Research Institute (ETRI) funded by the Korean government [23ZH1100, Study on 3D Communication Technology for Hyper-Connectivity]. "

1. Introduction

Unmanned aerial vehicles (UAVs) are attracting attention as a key element of new radio (NR) systems because of their high-altitude and mobility characteristics, specifically because they can exceed the limits of terrestrial networks. UAVs are also being used in diverse environments such as commodity delivery, natural disaster monitoring, and remote-control platforms because of their flexibility and mobility [1-3]. Additionally, UAVs can facilitate communication between aviation and ground networks.

Recently, network usage has increased with the increased demand for data. Consequently, the range of communication frequencies has been extended to include high-frequency millimeter waves to accommodate the increased usage and solve the data traffic problem [4]. In this context, UAVs with high-speed and high-altitude characteristics have emerged as a promising solution. UAVs can access data at high speeds; hence, in NR systems, where UAVs are used as base stations (BSs) or user equipment (UE), they can facilitate high-speed transmission.

However, high-altitude UAVs are likely to be affected by intercell interference from other BSs or UE because the line-of-sight (LOS) probability increases. For the mitigation of such interference, research on beamforming technology is being conducted, and beam selection algorithms for selecting the optimal beam to maximize the transmission efficiency are being studied. A commonly used method involves selecting the optimal beam on the basis of the perfect channel state information under the assumptions of accurate channel estimation and channel feedback [5]. However, this method introduces overheads because the users' environments and channel status information need to be compared individually. To reduce the overhead, a study proposed a compressed-sensing-based beam selection method rooted in the scarcity of millimeter-wave channels [6]. This method can reduce the execution time by estimating the location or direction of the UE. In addition, a method of using a fingerprint storing location-based channel information or received signal strength is mainly used to help users select an appropriate beam at a specific location. In [7], to increase the efficiency of beam tracking, a method of tracking the beam using a fingerprint storing channel information by mapping the beamforming gain and the user position was proposed. In [8], a technique for selecting different beams to eliminate interference between users, which involved the use of group-based fingerprint information was proposed. In [9], we proposed a method of selecting an appropriate beam according to multiple location-based fingerprints collected considering traffic density.

In this paper, for a UAV-enabled cellular cooperative system, we propose an algorithm to select the optimal beam on the basis of the user type by using a fingerprint database based on users' locations. The proposed algorithm can be divided into a location-based fingerprint database construction process and a cooperative beam selection process. During the construction of the fingerprint database, for improving the performance of UE strongly affected by interference, such as those located at the cell edge or at high altitudes, both their optimal-beam-related information and interference-beam-related information are stored. During the cooperative beam selection process, instead of comparing individually with the existing status information, the optimal beam for the user's location is selected by simultaneously using the optimal beam information and interference beam information from the location-based fingerprint database created in the previous process.

The remainder of this paper is organized as follows. Section 2 defines the system model and introduces the applied channel model. Further, Section 3 presents the cooperative beam selection algorithm, which involves the use of a location-based fingerprint database, for a

cellular cooperative system. Next, Section 4 discusses the performance of the algorithm in simulation environments and presents the simulation results. Finally, the conclusions of this study are provided in Section 5.

2. Cellular-Cooperative Downlink System Model and Channel Model

2.1 Cellular-Cooperative Downlink Systems

In this study, we considered NR downlink systems in which terrestrial base stations (T-BSs) support multiple terrestrial UE (T-UE) and unmanned aerial vehicle-user equipment (UAV-UE) in a multicell environment as depicted in **Fig. 1** [10]. The network comprised hexagonal cells, each of which was divided into three sectors. Each cell contained a T-BS that supported multiple T-UE and UAV-UE in the downlink system. In particular, we considered all T-UE to be outdoors, not inside a building, and all UAV-UE to be randomly distributed between the altitudes of 50 and 300 m [11-13]. Location information is essential for applying the proposed algorithm, and the propagation environment of the signal in the case of indoor T-UE is more complicated than that in the case of outdoor T-UE [11-13], which can cause outliers and noise in calculating the normal received signal strength, making it difficult to calculate the exact value. Therefore, an efficient location-based fingerprint database construction method that can remove data outliers and noise is needed [14], which is left as a future research project. This paper only considers outdoor T-UE and UAV-UE.

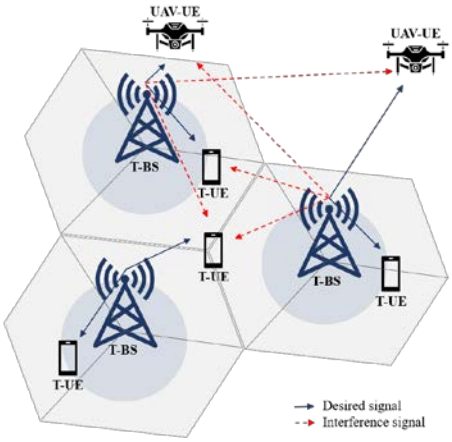

Fig. 1. Cellular-cooperative downlink systems.

Each T-BS has N_{BS} antennas and N_{RF} radio-frequency (RF) chains, with each antenna supporting K T-UE and UAV-UE [15].

$$y_{bk} = \hbar_{bbk} w_b s_b + \sum_{i \neq b} \hbar_{ibk} w_i s_i + \epsilon_{bk}. \tag{1}$$

The signal received by the kth user in the bth cell can be expressed as (1), where, $w_b \in C^{N_{BS} \times K}$ denotes a digital precoding matrix, $s_b \in C^{K \times 1}$ ($s_b = [s_{b,1}, \ldots, s_{b,K}]^T$) represents a data symbol vector corresponding to the bth cell, $s_{b,k}$ is the data symbol of the kth UE in the bth cell, $\epsilon_{bk} \sim CN(0,\ \sigma_\epsilon^2)$ is the thermal noise, and $\hbar_{ibk} \in C^{1 \times N_{BS}}$ denotes the channel vector

between the *i*th T-BS and *k*th UE in the *b*th cell.

$$\mathbf{U_{ULA}}(\mathrm{N_{BS}}) = \left[\mathrm{u}_0, \mathrm{u}_1, \dots, \mathrm{u}_{\mathrm{N_{BS}}-1}\right], \tag{2}$$

$$\mathrm{u}_b = \frac{1}{\sqrt{\mathrm{N_{BS}}}}\left[1, e^{j\frac{2\pi}{\mathrm{N_{BS}}}b}, e^{j\frac{2\pi}{\mathrm{N_{BS}}}2b}, \dots, e^{j\frac{2\pi}{\mathrm{N_{BS}}}(\mathrm{N_{BS}}-1)b}\right]^T, \tag{3}$$

$$\mathbf{U_{UPA}} = \mathbf{U_{ULA}}\left(\mathrm{N_{BS}^H}\right) \otimes \mathbf{U_{ULA}}\left(\mathrm{N_{BS}^V}\right). \tag{4}$$

In an existing massive multiple-input multiple-output system, an RF chain is required for each antenna; therefore, an antenna is configured as a lens to reduce the number of RF chains required. An array of such lens-type antennas acts as a discrete Fourier transform (DFT) vector in space, which includes an array steering vector. The spatial DFT codebook of a uniform linear array (ULA) with $\mathrm{N_{BS}}$ antennas can be expressed as (2), and the parameter u_b, which denotes the *b*th codeword, is given by (3). By using the Kronecker product, we can expand the ULA codebook to obtain a codebook suitable for a uniform planar array (UPA) with $\mathrm{N_{BS}}$ ($= N_{BS}^H \times N_{BS}^V$) antennas, expressed as (4).

2.2 Channel Model

In this study, a Third-Generation Partnership Project (3GPP)-based UAV channel model was employed, and a spatial channel model (SCM) was used between the T-BS and UE [11], [13]. The parameters of the statistical model employed in the SCM were calculated statistically by performing repeated measurements. Furthermore, the parameters of the deterministic model employed in the SCM were calculated using a ray-tracing model that mathematically expressed and tracked propagation characteristics [15-16]. Among them, a geometry-based stochastic model that utilized both these models was used in this study.

When the aforementioned SCM model is used, the channel parameters should be set according to the scenario considered. In this study, we considered the UMa-AV scenarios. Detailed model descriptions can be found in the papers listed in the 3GPP bibliography; therefore, they have been omitted from this paper [11], [13]. The process of generating channel correlation coefficients is useful for designing a network for a scenario and computing the general parameters of large-scale fading models, such as path loss and shadow fading models. Next, small-scale parameters such as cluster power and arrival angle should be set, and the channel correlation coefficients should be calculated. The path-loss and shadow fading models used in this study correspond to the UMa scenario described in [11] and [13].

$$\tilde{\mathbf{H}} = \left[\tilde{\mathbf{h}}_\mathbf{1}, \tilde{\mathbf{h}}_\mathbf{2}, \dots, \tilde{\mathbf{h}}_\mathbf{K}\right] = \mathbf{UH} = \left[\mathbf{Uh_1}, \mathbf{Uh_2}, \dots, \mathbf{Uh_k}\right], \tag{5}$$

$$\tilde{\mathbf{H}}_\mathrm{b} \in C^{K\times K} = \tilde{\mathbf{H}}(\mathrm{m}, :)_{\mathrm{m}\in\mathbf{S}}, \tag{6}$$

$$\tilde{\mathbf{w}}_\mathrm{b} = \alpha\tilde{\mathbf{H}}_\mathrm{b}(\tilde{\mathbf{H}}_b^H\tilde{\mathbf{H}}_\mathrm{b})^{-1}. \tag{7}$$

To construct a channel vector in this system, considering (2) in Subsection 2.1, the spatial DFT codebook of a ULA must be expanded to the form of UPA as given by (4). Moreover, the channel vector can be represented by the product of the UPA codebook vector **U** and the channel vector **h** using the SCM channel model. Referring to (5), $\tilde{\mathbf{h}}_{\mathrm{k}}$ ($\mathrm{k} = 1,2,\ldots,K$) denotes the beam space channel vector of the *k*th UE. If a T-BS has *K* RF chains ($N_{RF} = K$) and uses an antenna array configured as a lens, a reduced-dimensional channel model should be formulated. Therefore, when using such an antenna array, the channel model can be expressed as (6), where ***S*** represents the set of selected beam indexes. In this study, a simple zero-forcing (ZF) precoder was used as a digital precoder; the dimensionally reduced ZF precoding matrix $\tilde{\mathbf{w}}_{\mathrm{b}}$ ($\tilde{\mathbf{w}}_{\mathrm{b}} \in C^{K\times K}$) is given by (7), where α is a scaling constant.

3. Cooperative Beam Selection Algorithm Using Location-based Fingerprint Database in Cellular Cooperative Systems

Herein, we propose an algorithm for selecting the optimal beam such that T-UE at the edge of a cell or UAV-UE at a high altitude is less affected by interference from other cells.

The algorithm can be divided into two stages. The first stage involves creating a location-based fingerprint database containing necessary information about various types of UE, which are classified using a criterion proposed herein. In the second stage, interference between cells is mitigated by using the constructed database. In the cooperative beam selection process, the amount of information exchanged between T-BSs affects resource utilization, which directly determines the cost of the system. However, our optimal beam selection algorithm is efficient because it reduces the amount of resources required for information exchange according to user classification.

3.1 Location-Based Fingerprint Database Construction

A location-based fingerprint database was constructed for both T-UE and UAV-UE positioned in each cell. During the construction of the database, data on UE location, serving cell ID, and optimal beam ID were stored, and in the case of UE susceptible to intercell interference, interference-related data were also stored.

$$projection - distance = 3D - distance \times \cos(\psi). \tag{8}$$

Before explaining the specific process of creating a fingerprint database, we propose criteria for UE classification. First, UE were classified into ground user, T-UE, and aerial user UAV-UE. We used a hexagonal cell network structure with inter site distance (ISD) = 500 [m]. We approximated hexagonal cells inside a circle with a radius of 250 [m] for computational convenience. The critical radius at which the area ratio of the center and edge of a cell was 1:1 was determined to be 175 [m]. The space covered by a circle of radius 175 [m] in a cell was termed cell-center two-dimensional (2D) space, and the space outside this circle inside the cell was defined as cell-edge 2D space (illustrated in **Fig. 2**). Accordingly, if the projection distance between the T-UE and T-BS, calculated using (8), was less than 175 [m], the T-UE was classified as cell-center T-UE; if it was greater than 175 [m], the T-UE was classified as cell-edge T-UE. All the parameters used in (8) are illustrated in **Fig. 3**.

In addition, UAV-UE were classified as cell-center UAV-UE and cell-edge UAV-UE by using the aforementioned projection distance of 175 [m] between the UAV-UE and T-BS. However, because UAV-UE are airborne, a three-dimensional (3D) space should be considered.

Therefore, as shown in **Fig. 2**, for UAV-UE, the cell-center and cell-edge 3D spaces were demarcated using a cylindrical column with a base radius of 175 [m].

Furthermore, because UAV-UE are located at different altitudes in 3D space, the LOS probability varies significantly with altitude. Therefore, it is necessary to consider the altitude. The proposed algorithm accordingly specifies a certain threshold altitude. If the altitude of the UAV-UE is higher than the threshold altitude, the probability of the UAV-UE being affected by intercell interference is high; in such a case, even if the UAV-UE is in the cell-center 3D-space, it is considered to be a cell-edge UAV-UE.

The following is a process of constructing beam information from a fingerprint database [15]. The beam selection process is divided into beam sweeping, beam measurement, beam determination, and beam reporting. First, beam sweeping transmits a previously known beam to cover a large space and then identifies the most optimal beam at a specific location along with the interference beam most affected by neighboring cells. Further, during the beam measurement process, the signal received at the specific user location is measured, and the optimal beam is determined for each location according to the measured value. Therefore, identifying the optimal beam ID is the same as selecting a beam with the largest channel vector norm ($|\tilde{\mathbf{h}}_{\mathbf{K}}|$) from the codebook **U** by calculating (5) using exhaustive search. In the case of users who are vulnerable to interference, interference-related information should also be stored; in this case, similar to the previous case, the exhaustive search method can be employed by using a channel vector ($\mathbf{h}_{\mathbf{k}}$) from a neighboring cell.

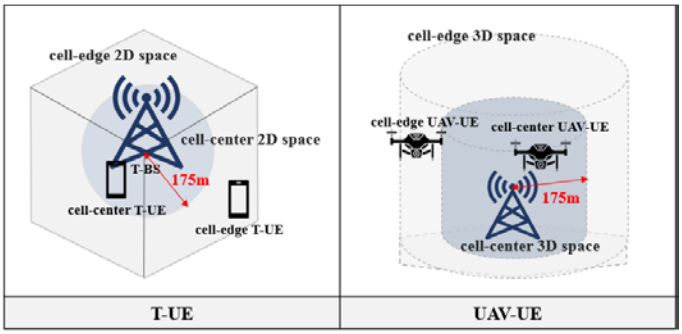

Fig. 2. Classification of UE types.

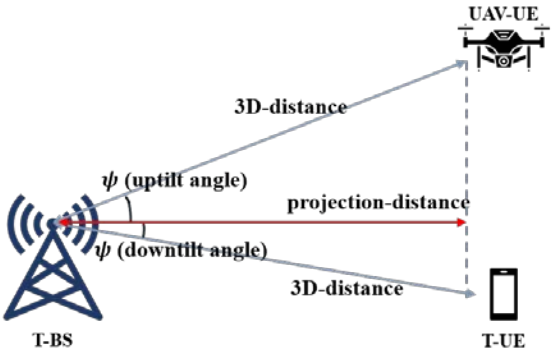

Fig. 3. Projection-distance measurement method.

In summary, the fingerprint database of a cell was constructed by considering the locations of all the T-UE and UAV-UE in the cell, and the locations of the UE and the optimal beam ID were recorded as the measurement contents. In the case of UE, which were strongly affected by interference, because interference-related information should be stored, the IDs of the interference cell and the corresponding interference beam were also stored.

Table 1. Example of fingerprint database.

UAV-UE									**T-UE**								
Cell-center			**Cell-edge**						**Cell-center**			**Cell-edge**					
P_1	...	P_A	P_{A+1}		...	P_{A+n}			p_1	...	p_B	p_{B+1}		...	p_{B+T}		
B_1^{opt}	...	B_A^{opt}	B_{A+1}^{opt}		...	B_{A+n}^{opt}			b_1^{opt}	...	b_B^{opt}	b_{B+1}^{opt}		...	b_{B+T}^{opt}		
			$\tilde{C}_{A+1}^{I\_1}$	$\tilde{B}_{A+1}^{I\_1}$	...	$\tilde{C}_{A+n}^{I\_1}$	$\tilde{B}_{A+n}^{I\_1}$					$\tilde{c}_{B+1}^{I\_1}$	$\tilde{b}_{B+1}^{I\_1}$	...	$\tilde{c}_{B+T}^{I\_1}$	$\tilde{b}_{B+T}^{I\_1}$	
			$\tilde{C}_{A+1}^{I\_2}$	$\tilde{B}_{A+1}^{I\_2}$	...	$\tilde{C}_{A+n}^{I\_2}$	$\tilde{B}_{A+n}^{I\_2}$					$\tilde{c}_{B+1}^{I\_2}$	$\tilde{b}_{B+1}^{I\_2}$	...	$\tilde{c}_{B+T}^{I\_2}$	$\tilde{b}_{B+T}^{I\_2}$	

Table 1 presents an example of a fingerprint database of a cell. The UE were first divided into UAV-UE and T-UE and then into cell-center UE and cell-edge UE. For the cell-center UE, only optimal-beam-related information was stored, and for cell-edge UE, interference-related information was stored along with optimal-beam-related information. In this study, if the altitude of a UAV-UE was greater than the arbitrarily specified threshold altitude, it was considered to be strongly affected by interference and stored in the cell-edge area in the fingerprint database, even if it was located in the cell-center 3D space. For the UAV-UE, let P_a $(a = 1, 2, \dots, A, A+1, \dots, A+n)$ represent the fingerprint location and B_a^{opt} $(a = 1,2, \dots, A, A+1, \dots, A+n)$ represent the optimal beam ID at the said fingerprint location. As discussed in the next section, in this study, interference-related information was exchanged using the intra-joint transmission (intra-JT) method. Let $\tilde{C}_a^{I\_1}$ $(a = 1, 2, \dots, A, A+1, \dots, A+n)$ and $\tilde{B}_a^{I\_1}$ $(a = 1, 2, \dots, A, A+1, \dots, A+n)$ represent the ID of the strongest interference cell and the corresponding interference ID, respectively, and let $\tilde{C}_a^{I\_2}$ $(a = 1, 2, \dots, A, A+1, \dots, A+n)$ and $\tilde{B}_a^{I\_2}$ $(a = 1, 2, \dots, A, A+1, \dots, A+n)$ represent the ID of the second-strongest interference cell and the corresponding interference beam ID, respectively. The T-UE fingerprint database was constructed using the same rules as those used to construct the UAV-UE fingerprint database; however, there was a difference between the two databases: they were expressed in uppercase and lowercase letters for distinguishing between them.

We used the reference signal received quality (RSRQ) as a database measurement indicator [17]. This was because the information provided by the reference signal received power (RSRP) could be insufficient in the event of unstable handover or cell reselection. Using RSRQ instead of RSRP could prevent such a problem. Furthermore, RSRP considers only the signals from the serving cells received by the terminal, whereas RSRQ additionally considers the signals received from the target cells other than the serving cells, which facilitates load balancing.

$$\mathrm{RSRQ} = N \times \mathrm{RSRP}/\mathrm{NR} - \text{carrier RSSI}, \tag{9}$$

$$\xi_n = \mathrm{d_n} + \mathrm{c_n} + 10log(BW). \tag{10}$$

RSRQ refers to the quality of the received signal considering the number of resource blocks and is calculated using (9), where *N* denotes the number of resource blocks in the NR-carrier received signal strength indicator (RSSI) measurement bandwidth and RSRP denotes the magnitude of the signal from the serving cell; in particular, RSRP indicates the measured power value of one resource block. NR-carrier RSSI refers to the sum of all signals received by the terminal from the target cell and those received from the serving cell, i.e., the total received power within the measurement bandwidth of *N* resource blocks. The signal received from the serving cell uses the RSRP value, and the signal received from a target cell other than the serving cell is determined on the basis of the altitude. Because the LOS probability increases with a UAV-UE's altitude, the UAV-UE may receive a signal from multiple target cells. Therefore, the reception signal from the target cell is classified using the threshold altitude, which is one of the adjustment variables mentioned in the previous section. If the altitude of the UAV-UE is less than the threshold altitude, its probability of being affected by nearby cells is considered to be low, and the signals received from the three nearest cells are classified as signals from target cells. Conversely, if the altitude is greater than the threshold altitude, the LOS probability is high, and interference signals may be received from six nearby cells. Accordingly, the signals received only from these six cells are divided into signals from the target cells. In addition to the magnitude of the received signal, components such as interference and noise should be considered. In the case of interference, in this study, only the interference that had a strong effect was considered in the calculation [9], and path loss and shadowing were calculated as components of interference. The noise power ξ_n was calculated using (10), which accounts for the thermal noise density (d_n), received noise figure (c_n), and bandwidth. The received noise figure (c_n) was 9 [dB], and the thermal noise density (d_n) was -174 [dBm/Hz].

3.2 Cooperative Beam Selection Algorithm According to User Classification.

$$P_o^* = \underset{a \in 1,\ldots,A+n}{\operatorname{argmin}} |P_o - P_a|^2 \tag{11-1}$$

$$p_o^* = \underset{a \in 1,\ldots,B+T}{\operatorname{argmin}} |p_o - p_a|^2 \tag{11-2}$$

The location information of UE can be used easily because of the high-level Global Positioning System modules built into them. Furthermore, the T-BS checks the received UE location information against the measured location information in the fingerprint database. The checking process is performed at a point where the error between the actual UE location and the location recorded in the fingerprint database is minimum as expressed by (11). Here, P_o is the current location of the UE and P_a is the location recorded in the fingerprint database. Consequently, the matched location (P_o^*) can be obtained at the point with the smallest square error between the two values. Equation (11-1) is for UAV-UE, while (11-2) is for T-UE. The definitions of p_o^*, p_o, and p_a in (11-2) are the same as those in (11-1), but lowercase letters are used in (11-2) for distinguishing them.

After the checking process is completed, a fingerprint database corresponding to the location (P_o^* or p_o^*) is created, and the serving cell and optimal beam IDs stored in the database can be used. In the case of UE that are susceptible to interference, interference-related information may be used. Therefore, the fingerprint database of matched UE indicates the type of UE. In the case of high-altitude UAV-UE or cell-edge UE, interference-related information can also be used.

$$SINR_{Coop.} = \frac{\sum_{c\in C} 10^{\frac{\xi_c}{10}}}{\left(\sum_{i\in B} 10^{\frac{\xi_i}{10}}\right) - \sum_{c\in C} 10^{\frac{\xi_c}{10}} + N_0} \tag{12}$$

$$SINR_{non-Coop.} = \frac{10^{\frac{\xi_b}{10}}}{\left(\sum_{i\in B} 10^{\frac{\xi_i}{10}}\right) - 10^{\frac{\xi_b}{10}} + N_0} \tag{13}$$

First, if the T-UE is identified as a cell-edge T-UE, it is more likely to be affected by interference compared to cell-center T-UE. Therefore, to improve the performance of cell-edge T-UE, we used the joint transmission (JT) method to exchange interference-related information stored in the fingerprint database for assisting with beam selection; this process is called the "Coop. method," where "Coop." is the abbreviation of "cooperation." In the Coop. method, multiple nearby cells cooperate to share stored information and select the optimal beam by jointly transmitting the related data to the UE. In this case, because the interference signal of the neighboring cell may also be used, interference from the neighboring cell may be reduced [15]. When the Coop. method is used, the signal-to-interference-plus-noise ratio (SINR) is determined using (12), and when the Coop. method is not used, the SINR is determined using (13). Here, ξ_a represents the power received from cell a, B represents the set of BSs, and C represents the set of JT-BSs. Therefore, according to (12), the Coop. method improves the reception power and reduces interference, thereby improving the performance.

The same holds true for UAV-UE. As mentioned, cell-center UAV-UE and cell-edge UAV-UE were distinguished by considering their altitude and location information, such as cell-center 3D space and cell-edge 3D space. The Coop. method was applied only to the UAV-UE in cell-edge 3D space, which were susceptible to interference, to reduce the effect of interference, improve signal performance, and reduce the amount of resources required for information exchange.

The proposed algorithms for location-based fingerprint database construction and optimal beam selection are presented in **Figs. 4** and **5**, respectively.

Algorithm 1 (offline) Location-based Fingerprint DB Construction

Input : UE Type, T-BS & UE location grid, RSRQ
Output : Location-based Fingerprint DB
(Offline) Location-based Fingerprint DB Construction

```
if UE Type == T-UE
    Measure projection-distance using 3D-distance and downtilt angle between T-BS and T-UE
    if projection-distance < 175m (*called cell-center T-UE)
        Construct fingerprint DB for optimal beam info.
    else (*called cell-edge T-UE)
        Construct fingerprint DB for optimal & interference beam info.
    end
else
    if UE altitude > = altitude_threshold
        Construct fingerprint DB for optimal & interference beam info.
    else
        Measure projection-distance using 3D-distance and uptilt angle between T-BS and UAV-UE
        if projection-distance < 175m (*called cell-center UAV-UE)
            Construct fingerprint DB for optimal beam info.
        else (*called cell-edge UAV-UE)
            Construct fingerprint DB for optimal beam info. & interference beam info.
        end
    end
end
```

Fig. 4. Location-based fingerprint database construction algorithm.

Algorithm 2 (online) Cooperative Beam Selection

Input : Location-based Fingerprint DB, New UE
Output : Optimal beam info.
(Online) Cooperative Beam Selection

```
Calculate error of location by exhaustive search using fingerprint DB
Find the best-matched DB
if UE Type == T-UE
    if UE Type == center-UE
        Select optimal beam info.
    else
        Exchange interference beam info. using beam cooperation
        Select optimal beam info.
    end
else (*called UAV-UE)
    if UE altitude >= altitude_threshold
        Exchange interference beam info. using beam cooperation
        Select optimal beam info.
    else
        if UE Type == center-UE
            Select optimal beam info.
        else
            Exchange interference beam info. using beam cooperation
            Select optimal beam info.
        end
    end
end
```

Fig. 5. Cooperative beam selection algorithm.

4. Simulation Results

This section presents the simulation environment and an analysis of the simulation results.

4.1 Simulation Setup

We considered an NR downlink system in which a T-BS located within each cell supported multiple UE, including UAV-UE and T-UE. The carrier frequency was set to 30 GHz on the basis of a bandwidth of 100 MHz. The "UMa-AV" scenario was considered, and the simulation was conducted on 19 cell systems divided into 3 sectors by system-level simulation. The specific parameters used in the experiment are listed in **Table 2**. The simulation environment was designed by referring to [9].

The SINR cumulative distribution function (SINR CDF) and spectral efficiency cumulative distribution function (SE CDF) were used as performance analysis metrics in the downlink-system-based simulations.

Table 2. Simulation parameters.

Parameters	Values
Cell layout	ISD = 500m, hexagonal grid, 19 cells, 3 sectors/cell
Carrier frequency (GHz)	30
Bandwidth (MHz)	100
T-BS Tx power (dBm)	35
Antenna configuration	T-BS : (UPA) 8 × 8
BS Tx power	T-UE : single / UAV-UE : single
Modulation	QPSK
Scenario	UMa
T-BS height (m)	25
T-UE height (m)	1.5
UAV-UE altitude distribution	Uniformly distributed between 50m and 300m
Measure indicator	RSRQ
Classification indicator (cell-center / cell-edge)	Projection-distance
Numerology	2 (normal)
SCS [kHz]	60
Sub-frame [ms]	1
RB [kHz]	720
N_{SC} (=SCS/RB)	12
N_{RB}	132

N_{tot} (=$N_{SC} \times N_{RB}$)	1584
T_b	$1 / (60 \times 10^3)$
f_s	$60 \times 10^3 \times 2048$

4.2 Performance Evaluation and Analysis

Figs. 6 and **7** depict the results of a simulation conducted to determine the degree of interference depending on the ratio of cell-center UE to cell-edge UE before the proposed algorithm was applied. The number of UE per sector used in each of the graphs is presented in rows 1–3 of **Table 3**. In the performance analysis, SINR CDF and SE CDF were used.

Table 3. The Number of UEs per sector used in the cases shown in Figs. 6-9.

	T-UE		**UAV-UE**	
	Cell-center	**Cell -edge**	**Cell -center**	**Cell -edge**
Parameter 1	4	12	4	12
Parameter 2	8	8	8	8
Parameter 3	12	4	12	4
Parameter 4	8	8	8	8
Parameter 5	12	12	4	4
Parameter 6	16	16	0	0

Rows 1–3 of **Table 3** indicate that as Parameter 1 transitioned to Parameter 3, the number of UE located in the cell-edge region decreased. Because the cell-edge region was more strongly affected by interference than the cell-center region, Parameter 1 indicates worse performance than Parameter 3. As shown in **Figs. 6** and **7**, the performance improved in the order of Parameter 1, Parameter 2, and Parameter 3.

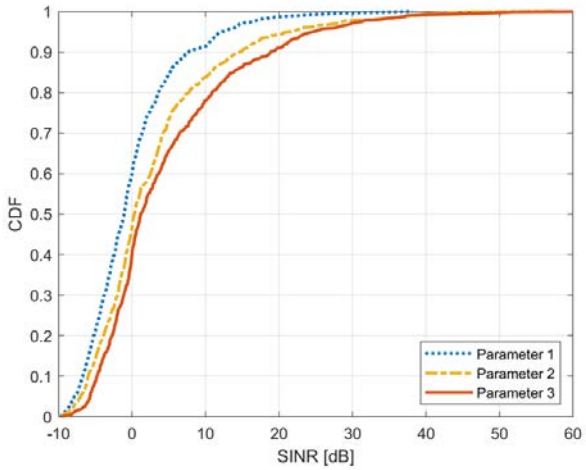

Fig. 6. Dependence of the SINR CDF on the ratio of the number of cell-center UE to the number of cell-edge UE.

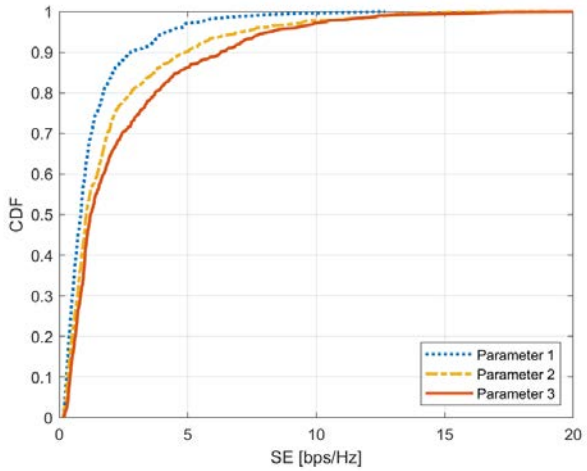

Fig. 7. Dependence of the SE CDF on the ratio of the number of cell-center UE to the number of cell-edge UE.

Figs. 8 and **9** present the results of a simulation conducted to understand the dependence of the degree of influence of interference on the number of UAV-UE before the application of the proposed algorithm. The numbers of UE per sector used in each of the graphs are listed in rows 4–6 of **Table 3**. The number of UAV-UE was adjusted first according to each graph, and the number of T-UE was adjusted to match the number of all UE by sector consistently. In this case, the ratio of the number of cell-center UE to the number of cell-edge UE was set to 50% for both T-UE and UAV-UE. Performance analysis was performed using the SINR CDF and SE CDF.

Rows 4–6 of **Table 3** reveal that as Parameter 4 transitioned to Parameter 6, the number of UAV-UE decreased. Because the UAV-UE at a high altitude is more strongly affected by interference than the T-UE, Parameter 4 indicates worse performance than Parameter 6. As shown in **Figs. 8** and **9**, the performance improved in the order of Parameter 4, Parameter 5, and Parameter 6.

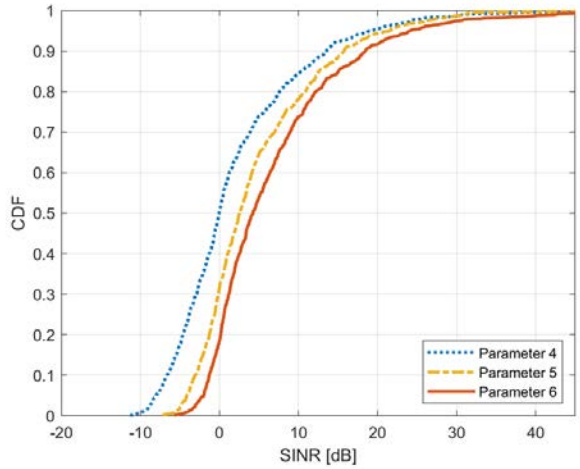

Fig. 8. Dependence of the SINR CDF on the number of UAV-UE.

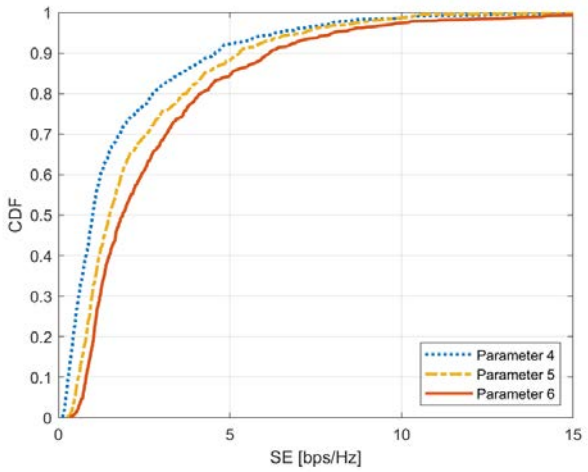

Fig. 9. Dependence of the SE CDF on the number of UAV-UE.

Figs. 11–14 show the results of several simulation cases performed to compare and analyze the performance of the proposed technique. In Category 1, T-UE were those to which the proposed Coop. method was not applied, and in Category 2, T-UE were those cell-edge T-UE to which the Coop. method was applied, not cell-center T-UE. Furthermore, applying the proposed algorithm to UAV-UE requires a threshold altitude to be specified. Accordingly, the UAV-UE were classified into three cases, namely, Cases 1, 2, and 3, which represented UAVs with threshold altitudes of 300, 175, and 50 [m], respectively. If the altitude of a UAV-UE was greater than the threshold altitude, its probability of being affected by interference was considered to be high, and the Coop. method was applied to it. It is divided into two cases: Scheme 1 and Scheme 2. First, in Scheme 1, the Coop. method is not applied unconditionally. On the other hand, in Scheme 2, UAV-UE is divided into cell-center and cell-edge, and the Coop. method is applied only to cell-edge that is greatly affected by interference. For easy comprehension by the reader, these performance analysis scenarios are visually depicted in **Fig. 10**.

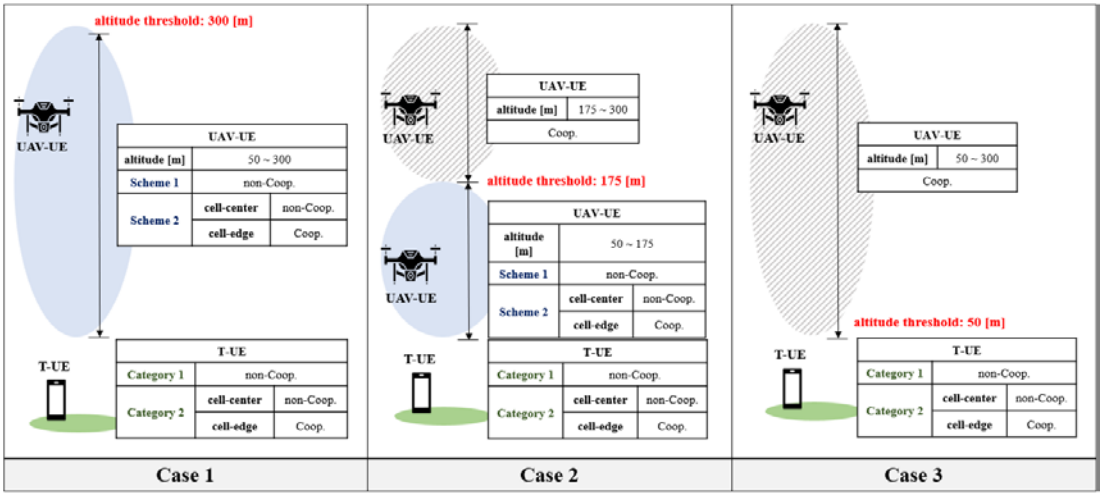

Fig. 10. Performance analysis scenarios.

Figs. 11 and **12** depict the results of the simulation in which the performance of Category 1 was analyzed. In other words, the Coop. method was not applied to T-UE but to a few UAV-UE. However, the Coop. method was applied to all the UAV-UE whose altitudes exceeded the threshold altitude. Conversely, when the altitude was lower than the threshold value, the analysis was divided into two schemes: Scheme 1 without the Coop. method and Scheme 2 where the Coop. method was applied only to the cell-edge UAV-UE. In Case 3, the UAV-UE were evenly distributed between 50 and 300 m, and the threshold altitude was set to 50 m. In this case, it was not possible to distinguish between Scheme 1 and Scheme 2; therefore, the Coop. method was applied to all the UAV-UE.

The simulation results presented in **Figs. 11** and **12** indicate that as the set threshold altitude was gradually reduced, the performance improved from Case 1 to Case 3. In addition, it was observed that Scheme 2, in which cell-edge and cell-center UE were separated and the Coop. method was applied to the cell-edge UE, performed better than Scheme 1. Therefore, "Category 1-Case 3" represented the optimal result because the Coop. method was applied to all the UAV-UE, resulting in performance improvements for all UAV-UE that were strongly affected by interference.

However, beam selection using the Coop. method led to heavy resource consumption for information exchange. Because this affected the system cost, it was efficient to apply the Coop. method to only a small number of UE, even if the performance was slightly reduced. Therefore, on the basis of **Figs. 11** and **12**, the performance of "Category 1-Case 2-Scheme 2" was found to be the closest to that of the optimal case. In other words, after setting the threshold altitude to 175 [m], we found that the application of the proposed algorithm to UAV-UE was efficient and did not significantly affect performance.

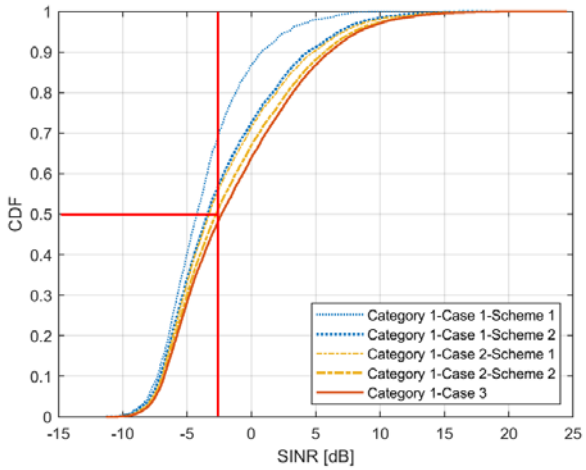

Fig. 11. Performance analysis of algorithms in Category 1 (SINR CDF).

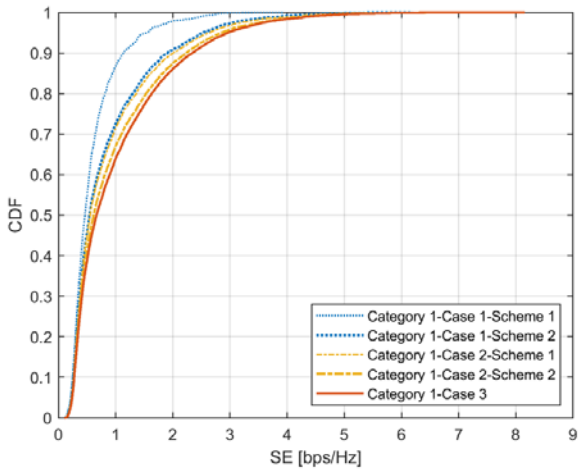

Fig. 12. Performance analysis of algorithms in Category 1 (SE CDF).

Figs. 13 and **14** present the performance analysis results of the proposed algorithm for Category 2, i.e., when the Coop. method was applied only to cell-edge T-UE and a few UAV-UE. The patterns in **Figs. 13** and **14** are similar to those of Category 1. Therefore, after setting the threshold altitude to 175 [m], we confirmed that application of the proposed algorithm to both UAV-UE and T-UE could lead to efficient beam selection without significant performance degradation.

The performance of Category 2 was superior to that of Category 1 as indicated by the CDF value of 0.5 reference SINR for "Category 1-Case 2-Scheme 2" and "Category 2-Case 2-Scheme 2" in **Figs. 11** and **13**, respectively. For the CDF value of 0.5, the SINR values of "Category 1-Case 2-Scheme 2" and "Category 2-Case 2-Scheme 2" were −3 and 0 [dB], respectively, which indicated the superior performance of "Category 2-Case 2-Scheme 2" because Category 2 applied the Coop. method to the cell-edge T-BS. In conclusion, when the proposed algorithm was applied to both T-UE and UAV-UE, it showed the best performance while being efficient in terms of system cost.

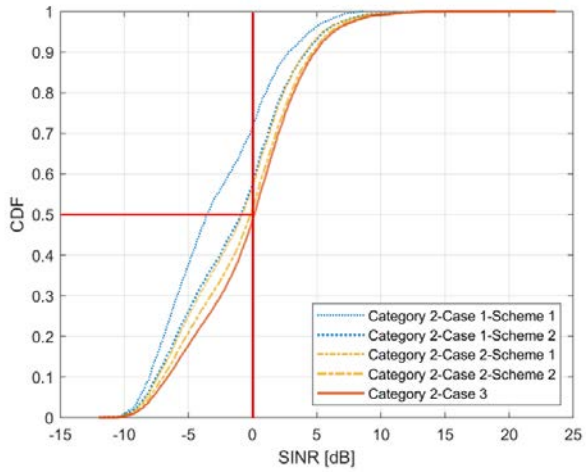

Fig. 13. Performance analysis of algorithms in Category 2 (SINR CDF).

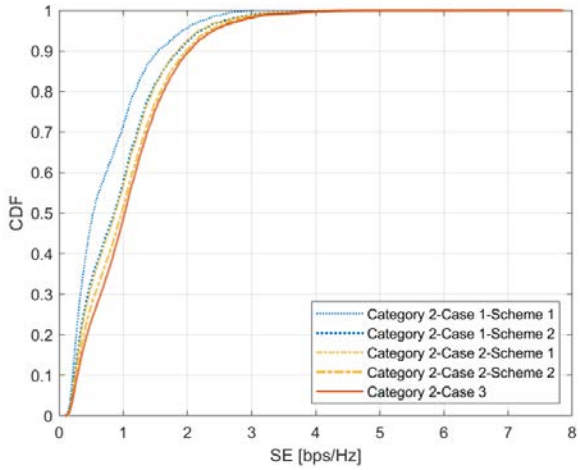

Fig. 14. Performance analysis of algorithms in Category 2 (SE CDF).

5. Conclusion

We propose a cooperative beam selection algorithm that uses a location-based fingerprint database for a UAV-based cellular cooperation system. The algorithm can be divided into an offline process of creating a location-based fingerprint database and an online process of selecting an optimal beam by using the fingerprint database. We divided the UE that were considerably affected by interference into ground-based UE and airborne UE, particularly UE located at the center and edges of a cell. Furthermore, the UAV-UE were classified according to their altitudes. The performance of UE with a high probability of being affected by interference was improved by facilitating cooperation between multiple cells for the sharing of interference-related information.

A system-level simulation conducted to analyze the performance of the proposed algorithm showed that the optimal beam was selected with high efficiency. From the performance analysis of the proposed algorithm in various scenarios, it was confirmed that the performance did not decrease significantly even if the proposed algorithm was applied to some users who were vulnerable to interference, not all the users. This implies that the proposed algorithm could reduce the effect of intercell interference and increase the performance of the desired signal. Furthermore, the proposed algorithm was found to be efficient in terms of reducing overheads and system cost. High efficiency was achieved by reducing the amount of resources required for information exchange.

References

[1] M. Mozafari, W. Saad, M. Benis, Y. H. Nam, M. Debbah, “A tutorial on UAVs for wireless networks: Applications, chal-lenges, and open problems,” *IEEE Commun. Surveys Tuts.*, vol.21, no.3, pp.2334-2360, 2019. Article (CrossRef Link)

[2] Z. Qadir, K. N. Le, N. Saeed, and H. S. Munawar, "Towards 6G Internet of Things: Recent advances, use cases, and open challenges," *ICT Express*, vol. 9, no. 3, pp. 296-312, June 2023. Article (CrossRef Link)

[3] F. Nait-Abdesselam, A. Alsharoa, M. Y. Selim, D. Qiao and A. E. Kamal, "Towards enabling unmanned aerial vehicles as a service for heterogeneous applications," *Journal of Communications and Networks*, vol. 23, no. 3, pp. 212-221, June 2021. Article (CrossRef Link)

[4] Y. Sim, S. Sin, J. Cho, S. Moon, Y. You, C. H. Kim and I. Hwang, "Beam Tracking Method Using Unscented Kalman Filter for UAV-Enabled NR MIMO-OFDM System with Hybrid Beamforming," *KSII Transactions on Internet and Information Systems (TIIS)*, vol. 17, no. 1, pp. 280-294, 2023. Article (CrossRef Link)
[5] E. Onggosanusi et al., "Modular and High-Resolution Channel State Information and Beam Management for 5G New Radio," *IEEE Communications Magazine*, vol. 56, no. 3, pp. 48-55, Mar. 2018. Article (CrossRef Link)
[6] J. Choi, "Beam Selection in mm-Wave Multiuser MIMO Systems Using Compressive Sensing," *IEEE Transactions on Communications*, vol. 63, no. 8, pp. 2936-2947, Aug. 2015. Article (CrossRef Link)
[7] R. Deng, S. Chen, S. Zhou, Z. Niu and W. Zhang, "Channel Fingerprint Based Beam Tracking for Millimeter Wave Communications," *IEEE Communications Letters*, vol. 24, no. 3, pp. 639-643, March 2020. Article (CrossRef Link)
[8] S. M. Moon, H. S. Kim, J. Y. Kim, D. J. Kim, and I. T. Hwang, "Beam Selection Scheme for Interference Cancellation in Beamspace Multi-user MIMO System," *Journal of the Institute of Electronics and Information Engineers*, vol. 57, no. 8, pp. 20-27, August 2020. Article (CrossRef Link)
[9] K. Satyanarayana, M. El-Hajjar, A. A. M. Mourad and L. Hanzo, "Deep Learning Aided Fingerprint-Based Beam Alignment for mmWave Vehicular Communication," *IEEE Transactions on Vehicular Technology*, vol. 68, no. 11, pp. 10858-10871, Nov. 2019. Article (CrossRef Link)
[10] IEEE 802.16m-08/004r2: IEEE 802.16m Evaluation Methodology Document (EMD). Article (CrossRef Link)
[11] 3GPP, “3rd Generation Partnership Project; Enhanced LTE support for aerial vehicles,” TR 36.777 V15.0.0, Jan. 2018. Article (CrossRef Link)
[12] 3GPP, “3rd Generation Partnership Project; 3D channel model for LTE,” TR 36.873 V12.7.0, Dec. 2017. Article (CrossRef Link)
[13] 3GPP, “3rd Generation Partnership Project; channel model for frequencies from 0.5 to 100 GHz,” TR 38.901 V16.1.0, Nov. 2020. Article (CrossRef Link)
[14] Zhang, Lingwen, Teng Tan, Yafan Gong, and Wenkao Yang, “Fingerprint Database Reconstruction Based on Robust PCA for Indoor Localization,” *Sensors*, vol. 19, no. 11, 2537, June. 2019. Article (CrossRef Link)
[15] S. M. Moon, H. S. Kim, Y. H. You, C. H. Kim, and I. T. Hwang, “Coordinated Millimeter Wave Beam Selection Using Fingerprint for Cellular-Connected Unmanned Aerial Vehicle,” *KSII Transactions on Internet and Information Systems (TIIS)*, vol. 15, no. 5, pp.1929-1943, May. 2021. Article (CrossRef Link)
[16] H. K. Chung, and K. C. Lee, “An Overview of Wireless Channel Model for B3G Mobile Communication,” *Electronics and Telecommunications Trends*, vol. 21, no. 3, p. 59-70, Jun. 2006. Article (CrossRef Link)
[17] 3GPP, “3rd Generation Partnership Project; NR; Physical layer measurements,” TS 38.215 V16.2.0, July. 2020. Article (CrossRef Link)

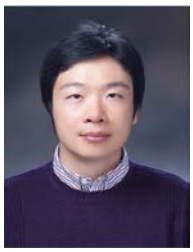

Jihyung Kim received his Ph.D. in Electrical and Electronic Engineering at the Yonsei University, Seoul, Republic of Korea, in 2007. Since 2007, he has been at the Electronics and Telecommunications Research Institute, Daejeon, Republic of Korea, where he is currently a Principal Researcher. His primary research interests include AI, RIS, UAV and NTN for 5G/6G mobile communications.

Yuna Sim received her B.S. in Electronics and Computer Engineering from Chonnam National University, Gwangju, Korea in 2022. She is currently pursuing her M.S. from the Department of ICT Convergence System Engineering, College of Engineering of Chonnam National University. Her research interests include digital communications, wireless communication systems, and next-generation mobile communications: 6G, artificial intelligence, multiple-input multiple-output systems, non-terrestrial networks, orthogonal frequency-division multiplexing, and unmanned aerial vehicles.

Sangmi Moon received the B.S., M.S., and Ph.D. degrees in Electronics & Computer Engineering from Chonnam National University, Gwangju, Korea, in 2012, 2014, and 2017 respectively. She was a visiting scholar in the School of Electrical Engineering and Computer Science, Oregon State University, USA, from Sep. 2017 to Feb. 2019. She was a postdoctoral research of the Department of Electronic Engineering, Chonnam National University, Korea, from Apr. 2018 to Feb. 2021. She is currently a Professor in the Department of IT Artificial Intelligence at Korea Nazarene University, Korea from Mar. 2021. Her research interests include 3D-MIMO, 3D-Beamforming, V2X, NTN, and artificial intelligence.

Intae Hwang received a B.S. degree in Electronics Engineering from Chonnam National University, Gwangju, Korea in 1990 and a M.S. degree in Electronics Engineering from Yonsei University, Seoul, Korea in 1992, and a Ph.D. degree in Electrical & Electronics Engineering from Yonsei University, Seoul, Korea in 2004. He was a senior engineer at LG Electronics from 1992 to 2005. He is currently a Professor in the Department of Electronic Engineering and Department of ICT Convergence System Engineering at Chonnam National University, Gwangju, Korea from 2006. His research interests include digital communication, wireless communication system, and next-generation mobile communication: MIMO-OFDM, V2X, NR-MIMO, NTN, and artificial intelligence.